Spin-dependent exciton formation rates in π-conjugated materials

2003 J. Phys.: Condens. Matter 15 R83

(http://iopscience.iop.org/0953-8984/15/3/202)

INSTITUTE OF PHYSICS PUBLISHING JOURNAL OF PHYSICS: CONDENSED MATTER

J. Phys.: Condens. Matter **15** (2003) R83–R107 PII: S0953-8984(03)33409-5

TOPICAL REVIEW

Spin-dependent exciton formation rates in π-conjugated materials

M Wohlgenannt[1] **and Z V Vardeny**[2]

[1] Department of Physics and Astronomy, University of Iowa, Iowa City, IA 52242, USA
[2] Physics Department, University of Utah, Salt Lake City, UT 84112-0830, USA

E-mail: markus-wohlgenannt@uiowa.edu

Received 29 October 2002
Published 13 January 2003
Online at stacks.iop.org/JPhysCM/15/R83

Abstract

π-conjugated compounds have been intensively studied for their use in 'plastic electronics', an alternative to inorganic semiconductor devices. In particular, research in the use of π-conjugated compounds as the active layer in electroluminescent devices has advanced rapidly: potential applications include e.g. flat, flexible display panels. In organic electroluminescent devices the annihilation of positive and negative charge carriers to the ground state proceeds via two fundamental steps: (i) formation of a neutral exciton, either spin singlet or spin triplet, and (ii) the radiative or non-radiative decay of the exciton. In most π-conjugated materials only the spin singlet exciton is emissive, and this is why the spin statistics of step (i) determines the maximum achievable electroluminescent efficiency. A number of recent studies indicate that exciton formation is spin dependent and that more singlets form in organic electroluminescent devices than what is expected from spin degeneracy. We review recent experimental and (to a lesser degree) theoretical results. In particular we focus on our own recent work, where we have measured the ratio, $r = \sigma_S/\sigma_T$, of the spin-dependent formation cross section, σ, of singlet (S) and triplet (T) excitons in π-conjugated oligomer and polymer films, using a spectroscopic/magnetic resonance technique. The experimental results reveal a distinct difference between exciton formation in molecular devices compared to polymer devices.

(Some figures in this article are in colour only in the electronic version)

Contents

1. Introduction

π-conjugated organic semiconducting materials, both small molecules and polymers, have attracted much scientific and commercial interest. Commercial interest is, to a large extent, motivated by the electroluminescent property of many π-conjugated compounds. Research in the use of π-conjugated compounds as the active semiconductors in light-emitting diodes has advanced rapidly (for a review see [1]). Organic light emitting devices (OLEDs) are now approaching efficiencies and lifetimes sufficient for the commercial market for e.g. large-area flexible displays or panel lighting. Highly efficient OLEDs can now be produced and become an attractive alternative to inorganic electroluminescence.

1.1. Organic electroluminescence

Organic electroluminescence (EL) was first reported for anthracene single crystals in the 1960s [2, 3]. Efficient EL was demonstrated in the 1980s by Tang and Van Slyke in two-layer sublimed molecular film devices [4]. These devices consisted of a hole-transporting layer of an aromatic diamine and an emissive layer of 8-hydroxyquinoline aluminium (Alq_3) (see figure 1). Indium tin oxide, ITO, is used as the transparent hole-injecting electrode, through which the EL is harvested, and a magnesium–silver alloy as the electron-injecting electrode. A large number of other molecular materials have been used as the charge-transporting or emissive layer in OLEDs.

Since the first report of metallic conductivities in 'doped' polyacetylene in 1977 [5], the science of electrically conducting, π-conjugated polymers has advanced very rapidly. As high-purity polymers have become available, a range of semiconductor devices have been investigated; these include transistors [6–10], photodiodes [11, 12] and OLEDs [13–17]. π-conjugated polymers derive their semiconducting properties by having delocalized π-electron bonding along the polymer chain. The π (bonding) and π^* (antibonding) orbitals form the valence and conduction bands, respectively, which support mobile charge carriers. EL from conjugated polymers was first reported in 1990 [13], using poly-p-phenylene-vinylene, PPV (PPV and other π-conjugated polymers used in OLEDs are shown in figure 1). Note the alternation of carbon–carbon single and double bonds, respectively, in both the π-conjugated small molecules (figure 1(a)) and the π-conjugated polymer backbones (figure 1(b)), which is the defining feature of π-conjugated compounds in general. The main advantage of using polymers, compared to small π-conjugated molecules, is their potential for large scale, low cost production using solution processing techniques.

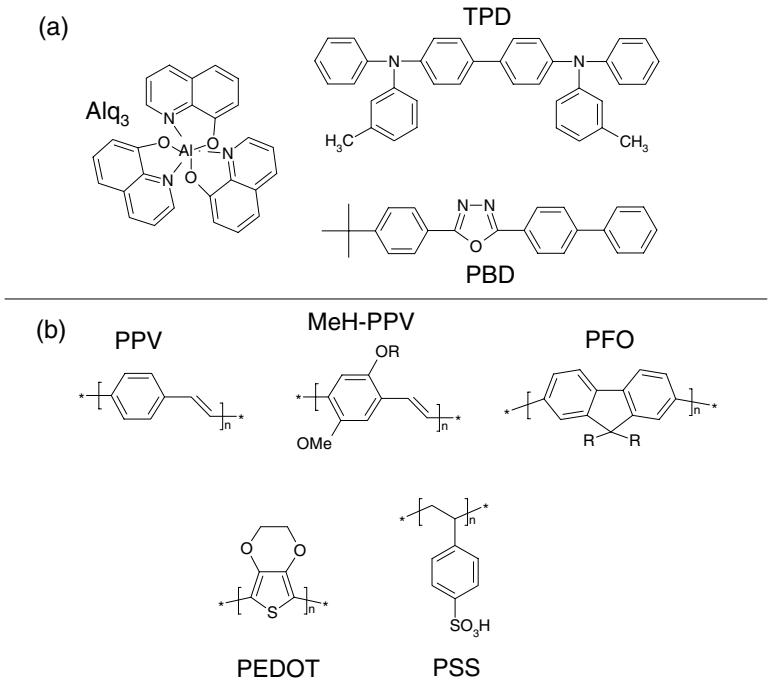

Figure 1. (a) Structures of some molecular semiconductors that have been used in thin-film electroluminescent devices. Alq_3 is used as an electron transport and emissive layer, TPD is used as a hole transport layer and PBD is used as an electron transport layer. (b) Polymers used in electroluminescent diodes. The prototypical (green) fluorescent polymer is poly(p-phenylene vinylene) (PPV). One of the best known (orange-red) solution processable conjugated polymers is MEH-PPV. Poly(dialkylfluorene)s (PFO) are blue-emitting, high-purity polymers, which show high luminescence efficiencies. 'Doped' polymers such as poly(dioxyethylene thienylene), PEDOT, doped with polystyrenesulfonic acid, PSS, are widely used as hole-injection layers.

The processes responsible for EL have been established in the early studies: electrons and holes (or rather, negative and positive polarons, since the electric charge couples strongly to the lattice in π-conjugated compounds) are first injected from the electrodes into the luminescent layer. The charge carriers then migrate through this layer and can form neutral, bound excitons, either spin singlet or triplet. The EL quantum efficiency, η_{EL}, can therefore be defined as a product of three factors [1, 18]: $\eta_{EL} = \eta_1\eta_2\eta_3$. η_1 is the fraction of emitted photons per optically active exciton formed, η_2 is the fraction of optically active excitons per total number of excitons and η_3 is the fraction of excitons formed per charge carrier flowing in the external circuit. In hydrocarbon materials usually only singlet states luminesce, whereas triplet states are usually non-emissive [19]. The maximum possible efficiency of fluorescence-based (only singlet states are emissive) OLEDs is therefore determined by the fraction of injected electrons and holes that recombine to form emissive spin-singlet excitons, rather than non-emissive triplet excitons.

1.1.1. Triplet harvesting. An assumption often employed until recently is that excitons are formed in the ratio of one singlet to three triplets, since only one singlet combination can be formed from the addition of two spin-1/2 charge carriers. However, the triplet state is three-fold degenerate (see figure 2). This is correct only if the process by which these excitons form were spin-independent, and then the maximum quantum efficiency, η_{max} of OLEDs

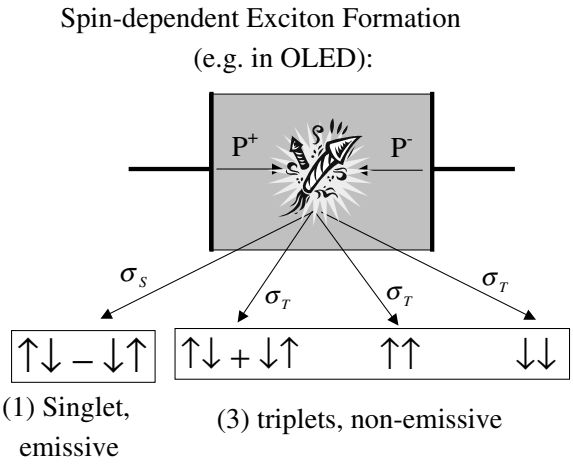

Figure 2. Spin-dependent exciton formation in OLEDs: the OLED device is schematically drawn as a single layer sandwich device. Upon application of forward bias, positive (P^+) and negative (P^-) charge carriers are injected. The charge carrier recombination is symbolized as a firework and the possible spin states for the resulting exciton are shown. Assigning different exciton formation cross-sections for the singlet (σ_S) and triplet (σ_T) channels allows for spin-dependent exciton formation.

would be limited to 25% [1]. The validity of this 25% spin degeneracy statistics was tested in an Alq_3 device, and a singlet fraction of (22 ± 3)% was found [20], in good agreement with expectations based on spin degeneracy statistics. Much research has therefore focused on finding schemes where both spin states, singlet and triplet excitons, can be used for light emission in OLEDs. Such schemes generally involve materials, primarily organometallic complexes, having significant spin–orbit coupling to promote the spin-flip needed for optical emission. The most prominent schemes for harvesting triplet excitons involve either using phosphorescence emission directly or using Förster transfer from the triplet state of the 'phosphorescent sensitizer' to the singlet state of a fluorescent guest complex [21]. Recent reports by Adachi *et al* have demonstrated an impressive internal phosphorescence efficiency of 87% [22]. In such devices the external efficiency is then mostly determined by the light out-coupling efficiency of the device. Very recently a new and potentially especially useful approach to the design of efficient electroluminescent materials has been proposed based on the discovery of a new mechanism for triplet harvesting [23]. Such devices use thermally activated triplet diffusion to trace amounts of covalently bound palladium sites, which are formed in a side reaction during polymer synthesis. The palladium then allows for phosphorescence emission.

The triplet harvesting scheme has proven very successful. However, a surprising recent discovery showed that, for electrical excitation in OLEDs made from π-conjugated polymers (rather than small molecules), a considerably higher number of singlet excitons are generated compared to what is expected from spin degeneracy statistics (i.e. 25%), and triplet harvesting might not always be necessary. The original report gave a singlet fraction of $\approx$50% [24] in a PPV-based device, and this report was soon confirmed by another laboratory [25]. To explain the large singlet yield the original report also speculated that either the exciton binding energy is weak or that singlet bound states are formed with higher probability than triplets. To our knowledge, all subsequent works consider the second alternative, since it is by now well established that the splitting between the lowest singlet and triplet excitons is typically 0.7 eV [19], so that at least the triplet exciton is strongly bound. The singlet exciton binding

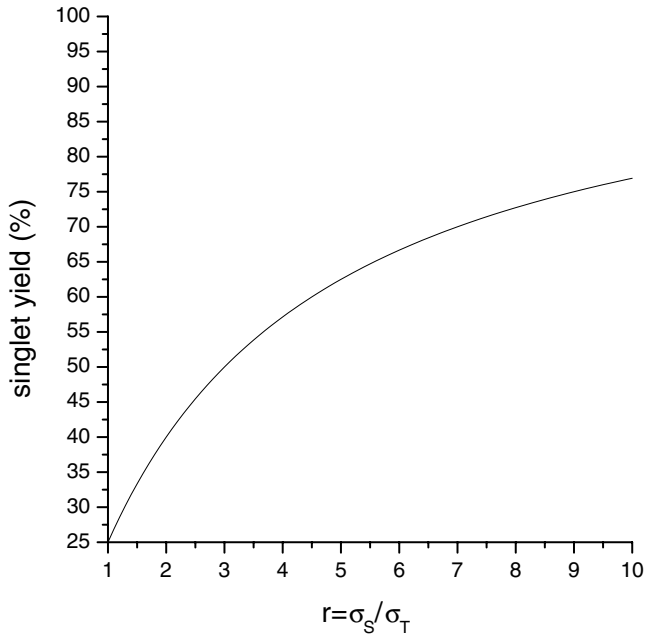

Figure 3. Dependence of the singlet yield on the ratio r of spin-dependent exciton formation cross sections.

energy is therefore also expected to be relatively large. The exact value for the singlet exciton binding energy has, however, remained a matter of intense discussion and ongoing research (see e.g. [26] for a review)

1.1.2. Spin-dependent exciton formation cross-sections. To accommodate the possibility that singlets and triplets form with different probabilities, Shuai *et al* [18] have introduced the spin-dependent exciton formation cross-sections, σ_S and σ_T, for singlet and triplet formation, respectively (see also figure 2). They also postulated that $\eta_2 = \sigma_S/(\sigma_S + 3\sigma_T)$ (see figure 3 for a plot of this function); for $\sigma_S = \sigma_T$ we retrieve $\eta_2 = 25\%$, the spin-statistical limit. Since the original report, a number of recent reports have indicated that η_{max} in OLEDs ranges between 22 and 83% [20, 24, 25, 27–30], and the reason for this variation is under investigation. Here we review these studies, focusing mainly on our recent work in this direction. The review is organized as follows. First (section 2), an overview of experimental methods is presented, followed by a detailed discussion of our spectroscopic/magnetic resonance experiments (section 2.1); thereafter measurements in phosphorescent OLEDs by the Cambridge group are summarized (section 2.2). Conclusions that emerged from the experimental work are discussed in section 2.3. Section 3 gives a brief account of important theoretical work and emphasizes the principal idea and major results of the various theoretical models. We will attempt to make connections between theoretical predictions and experimental results. The conclusions from both theory and experiment are presented in section 4. The appendix gives a detailed derivation of the formula $\eta_2 = \sigma_S/(\sigma_S + 3\sigma_T)$, connecting the spin-dependent exciton formation cross-sections and η_{max} in OLEDs. We note that this relationship depends on the presence of effective competing channels during exciton formation in OLEDs. Such competing channels in OLEDs have, to the best of our knowledge, not yet been explicitly identified.

2. Experimental work

Two entirely different experimental approaches have been employed to study spin-dependent exciton formation:

(i) Experiments that determine the ratio of the singlet/triplet exciton densities generated in 'live' OLEDs. Typical experimental techniques include measurements of the EL and photoluminescence quantum efficiencies. For fluorescent devices typically only the singlet emission can be studied: information on the triplet density is missing and rather involved models have to be employed to obtain the singlet/triplet ratio. Wilson *et al* [28] have recently shown that in some phosphorescent devices both singlet and triplet emission can be observed, and this allows more confident determination of the singlet/triplet ratio. In a different approach Dhoot *et al* [30] used measurements of triplet absorption in live OLEDs to infer the generated triplet density.

(ii) Experiments that measure the ratio r of the spin-dependent exciton formation cross-sections. Such experiments manipulate the spin state (using electron spin resonance) of the recombining charge carriers and measure the effect on charge carrier recombination and exciton formation rates and charge carrier and exciton populations. Such experiments 'aim' directly at the spin-dependent exciton formation process and should therefore allow direct conclusions to be drawn about the physics underlying the spin dependence of exciton formation. Such experiments [27, 29, 31] have thus far been performed only on thin films rather than 'live' devices.

2.1. Measurement of r using spectroscopic/magnetic resonance techniques

In this section we discuss the spectroscopic/magnetic resonance technique we used [27, 29, 31] to measure r in a large variety of π-conjugated polymer and oligomer thin films. These spectroscopic/magnetic resonance experiments are the main emphasis of this review; the experiments performed by Wilson *et al* [28] on live phosphorescent OLEDs will be discussed thereafter. Our technique uses both the photoinduced absorption (PA) and PA-detected magnetic resonance (PADMR) spectroscopies. We therefore studied *photogenerated* polarons in thin films rather than polarons injected into OLED devices. We note that in principle it is possible to use our technique directly in OLED devices, but it has been shown [32] that in such measurements electrode interface effects and transport effects make a quantitative interpretation very involved at best. Measurements on films are also less time-consuming, easier and more general (also non-luminescent materials can be studied), and this allowed us to study a large number of materials and examine the materials dependence of r. Once the material dependence of r is understood, this aids *a priori* selection of a π-conjugated material as the active layer for highly efficient OLEDs.

2.1.1. Experimental. The PA technique has been widely used in π-conjugated materials for studying long-lived photoexcitations with PA bands at subgap energies [33–40]. Two light beams are used in PA; one excites the sample film and the other probes the modulated changes, ΔT, in the optical transmission, T. For excitation typically a cw Ar^+ laser beam is used modulated with a chopper between 10 Hz and 10 kHz. CW PA is therefore sensitive only to processes that occur on a timescale between roughly 10 μs and 10 ms. In order to be able to study the polaron kinetics, the recombination processes are slowed down by measuring at low temperatures. Under typical experimental conditions the steady state density of photogenerated polarons is estimated to be $\approx 10^{17}$ cm^{-3}. Typically an incandescent tungsten–halogen lamp is

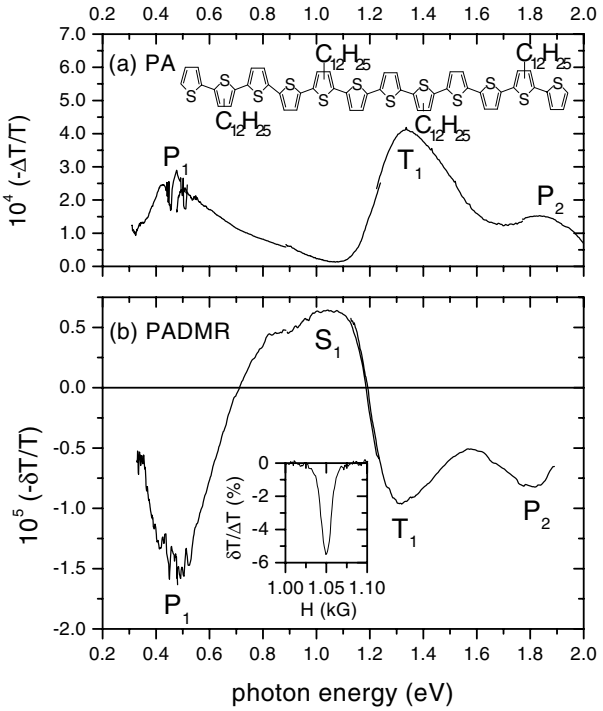

Figure 4. (a) The PA spectrum of 12 T (inset); (b) the PADMR spectrum at magnetic field $H = 1.05$ kG corresponding to $S = 1/2$ resonance (see inset in (b)). Both spectra (a) and (b) show two bands (P_1 and P_2) due to polarons. T_1 is due to triplet absorption. S_1 is assigned to singlets. The PA was measured at 80 K, excitation was by the 488 nm Ar^+ laser line (500 mW); the PADMR spectrum was measured at 10 K.

used for the probe beam. The PA spectrum ($\Delta\alpha$) is obtained by dividing $\Delta T/T$, where ΔT was measured by a phase sensitive technique, and $\Delta\alpha = -d^{-1}\Delta T/T = n\Sigma$, where d is the film thickness, n is the photoexcitation density and Σ is its optical cross-section. For probe photon energies below the cut-off wavelength of the glass bulb a Fourier transform infra-red (FTIR) spectrometer is typically used.

Thanks to a large number of previous PA studies in the literature, the nature of the long-lived photoexcitations as well as their characteristic absorption bands inside the optical gap are well understood and firmly established. The PA spectra of the films we have studied all show bands due to long-lived photogenerated charge carriers (polarons) and triplet excitons. Although the majority of photoexcitations are expected to be singlet excitons [26], they usually do not show up in cw spectroscopy, because of their much shorter lifetime. Figures 4(a) and 5(a) show typical PA spectra in oligomer and polymer films, respectively. Figure 4(a) is measured in a thin film of a soluble oligothiophene [41] (12 T, see figure 4(a), inset), whereas the spectrum in figure 5(a) is for methylated ladder type poly(para-phenylene) [42] (mLPPP, see figure 5(a), inset). In both spectra the characteristic two bands due to polarons (P_1 and P_2) are assigned, whereas the triplet exciton absorption is a single band (T_1). All films we have studied show a PA spectrum similar to those of figures 4(a) and 5(a). The transitions important in PA spectroscopy together with a schematic energy level diagram are shown in figure 6.

The effect of spin-dependent recombination on the PA bands in the photomodulation spectrum can be studied by the spin-1/2 PADMR technique [27, 29, 43–47]. In this technique

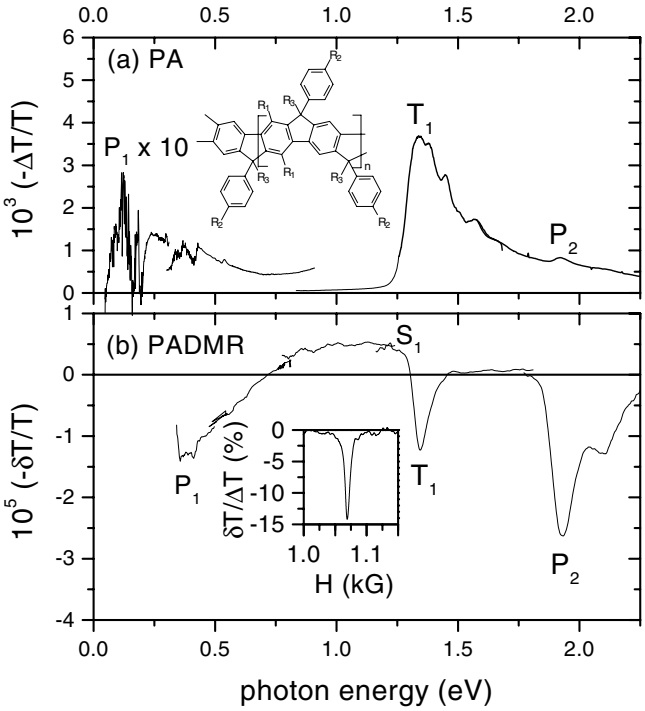

Figure 5. (a) The PA spectrum of mLPPP (inset); (b) the PADMR spectrum at magnetic field $H = 1.06$ kG corresponding to $S = 1/2$ resonance (see inset in (b)). Both spectra (a) and (b) show two bands (P_1 and P_2) due to polarons. T_1 is due to triplet absorption. S_1 is assigned to singlets. The PA was measured at 80 K, excitation was by the 457 nm Ar^+ laser line (300 mW); the PADMR spectrum was measured at 10 K.

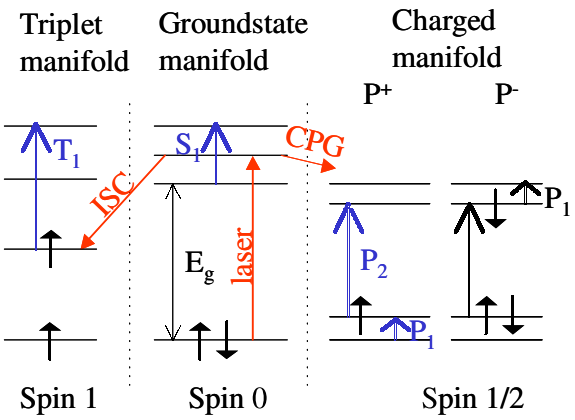

Figure 6. Schematic energy level diagram for photogenerated triplet excitons and polarons. For completeness the energy levels in the ground state manifold (ground state level together with neutral, spin singlet excitations) is also shown. The transitions important for cw PA spectroscopy and the intersystem crossing (ISC) and charge photogeneration (CPG) processes are assigned. E_g is the optical gap.

we measure the changes, δT, that are induced in ΔT by spin-1/2 magnetic resonance. δT is proportional to δn that is induced in the photoexcitation density, n (see below). Two types of PADMR spectra are possible: the H-PADMR spectrum where δT is measured at a fixed probe wavelength, λ, as the magnetic field H is scanned, and the λ-PADMR spectrum where δT is measured at a resonant H while λ is scanned. For the detailed description see [48]

The PLDMR technique [31, 49–53] is closely related to PADMR: PLDMR measures changes, δPL, induced in PL (rather than PA) upon magnetic resonance. We note that PA, PADMR and PLDMR can all be measured using the same set-up and under identical conditions, allowing accurate comparison between results of the three methods. The term 'optically detected magnetic resonance (ODMR)' is often used for both PADMR and PLDMR. We note that ODMR experiments are performed at low temperature (typically 10 K), mainly because of two reasons:

(a) the polaron lifetime is strongly temperature-dependent and is sufficiently long for study using cw spectroscopies only at temperatures below typically 100 K;
(b) the spin–lattice relaxation time is strongly temperature-dependent and becomes very long at low temperatures, such that the spin alignment is conserved during the modulation period of the experiments.

We also note that at low temperature the capture radius for charge-carrier recombination is large compared to the average distance between photogenerated polarons, so that oppositely charged polarons form recombination pairs.

In PA and PADMR charge-transfer (CT) or recombination reactions occur between neighbouring P^+ and P^-; the product of CT reactions are neutral excitons, either spin-singlet or triplet. The CT reaction rate R_P between spin parallel pairs ($\uparrow\uparrow$, $\downarrow\downarrow$) is proportional to $2\sigma_T$, whereas the CT reaction rate R_{AP} between spin antiparallel pairs ($\uparrow\downarrow$, $\downarrow\uparrow$) is proportional to $(\sigma_S + \sigma_T)$, where the proportionality constant is the same in both cases [27]. These relations are obtained as follows (see figure 2): antiparallel pairs may form either the $\uparrow\downarrow - \downarrow\uparrow$ (total spin singlet state) or $\uparrow\downarrow + \downarrow\uparrow$ combination (total triplet), whereas parallel pairs form only total triplet pairs ($\uparrow\uparrow$ or $\downarrow\downarrow$).

We have shown [27, 29, 31] that $\sigma_S > \sigma_T$ in π-conjugated compounds. Therefore $R_{AP} > R_P$ and spin parallel pairs prevail at steady state conditions (see figure 7 for a graphical illustration). Under saturated magnetic resonance conditions the polaron pair densities with parallel and antiparallel spins become equal (see figure 7). It then follows that the PADMR measurements detect a reduction, δN (which is proportional to δT), in the polaron pair density N (which is proportional to ΔT), since slowly recombining parallel pairs are converted to more efficiently recombining antiparallel pairs. At the same time the density of triplet excitons also decreases as a result of the decrease in the density of parallel polaron pairs, whereas the singlet exciton density increases as a result of the increase in the density of antiparallel polaron pairs. This paragraph is summarized in a graphical representation shown in figure 7.

The spin-1/2 PADMR spectra (figures 4(b) and 5(b)) clearly show the negative magnetic resonance response at P_1, P_2 and T_1, which are due to a reduction in the polaron and triplet densities, in agreement with our expectations. The PADMR spectra therefore directly prove $r > 1$ in these π-conjugated compounds. We also assign the positive PA band in the λ-PADMR spectra (S_1) to excess singlet exciton absorption expected from the above discussion.

Figure 8 shows the comparison between the PADMR spectrum of a polyfluorene (PFO) thin film measured at 10 K and the picosecond transient absorption spectrum measured on nominally the same film at 300 K [54]. It can be seen that the PADMR band S_1 and the singlet exciton absorption band PA_2 in the picosecond spectrum occur at similar spectral positions and have similar shape. This strengthens the assignment of S_1 to singlet exciton

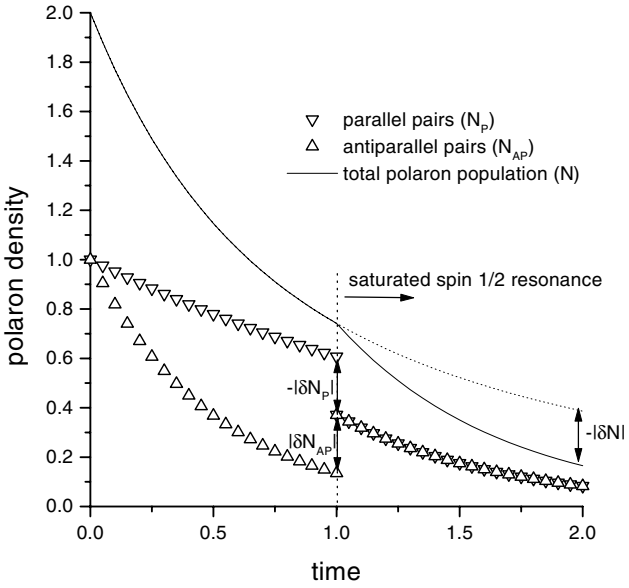

Figure 7. A graphical representation of the spin-dependent decay dynamics of polarons. The up-triangles (down-triangles) represent spin parallel (spin antiparallel) polaron pairs with density N_P (N_{AP}). The full curve represents the total population, N. The dynamics are drawn for $\sigma_S > \sigma_T$. At times larger than 1 saturated spin-1/2 electron spin resonance conditions ($N_P = N_{AP}$ for $t > 1$) are enforced and this leads to a reduction $-|\delta N|$ in N. $-|\delta N_P|$ leads to a reduction in triplets formed, whereas $|\delta N_{AP}|$ enhances the singlet population. For simplicity the dynamics is drawn for the case where polarons are photogenerated at time 0 using a laser pulse, whereas in the PADMR experiment polarons are generated at all times using a cw laser.

absorption. The PADMR band is, however, red-shifted by ≈0.2 eV with respect to the picosecond band. This red-shift of the cw band may be accounted for by spectral migration from the pico- to the millisecond time domains and/or a red-shift of the singlet absorption band between a measurement at 300 K (pump and probe spectrum) and 10 K (PADMR spectrum). However, more ultrafast pump and probe experiments have to be completed (especially at low temperature) to make this assignment definite.

2.1.2. Spin-dependent exciton formation probed by PLDMR spectroscopy. In addition to the PADMR band S_1 it is possible to probe the resonantly enhanced singlet population by means of the fluorescence emission, which originates from the singlet exciton. Therefore PLDMR studies were performed [31] on films of two representative π-conjugated polymers, namely PPV and regio-random poly(3-hexyl-thiophene) (RRa-P3HT). Films of these polymers show, at the same time, relatively large intensities for both PA spectrum and PL emission. In many other materials, since PA and PL are competing processes, either the PA or PL intensities are weak. A positive PLDMR spin-1/2 resonance that is a mirror image of the PADMR resonance is observed in all the films we have studied.

We have been able to advance the notion that the enhanced PL is a result of spin-dependent polaron recombination [31]. This can be shown by a comparison between the polaron recombination kinetics and the PLDMR signal kinetics. To this end the dependencies of the polaron PA and PLDMR signals on the laser intensity were studied [31]. Figure 9 shows the experimentally determined dependencies of PL, δPL and polaron PA band P_1 (where

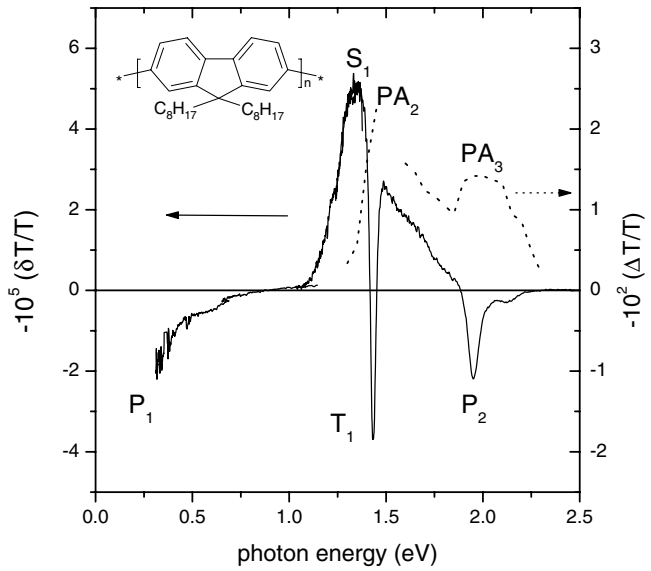

Figure 8. Comparison between PFO PADMR spectrum (full curve) at 10 K and transient absorption spectrum (broken curve) at 300 K and a delay of 15 ps. In transient absorption no reliable data could be obtained in the vicinity of the pump beam wavelength (≈1.5 eV). PA_2 in the transient absorption spectrum is due to singlet excitons, S_1 in the PADMR spectrum is assigned to cw absorption of the singlet excitons.

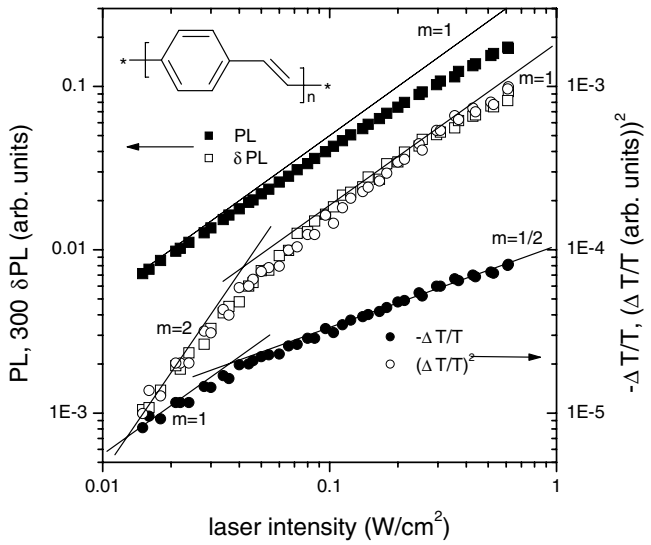

Figure 9. The laser intensity dependencies of the photoluminescence (PL, full squares), the magnetic resonance effect on the photoluminescence (δPL, open squares), the polaron PA band measured at 0.55 eV ($-\Delta T/T$, full circle) and its square (open circles, rescaled) in a PPV film measured at 10 K. The modulation frequency was 1 kHz.

$-\Delta T/T \propto N$) on the laser intensity, Φ, in a PPV film. We first discuss the polaron kinetics: figure 9 shows that the polaron PA signal scales as $\Phi^{1/2}$ at large Φ, which shows that polaron recombination follows a rate equation law with bimolecular recombination kinetics:

$$\frac{dN}{dt} = \eta\Phi - BN^2, \tag{1}$$

where B is the bimolecular recombination constant. Such a rate equation yields the $\Phi^{1/2}$ law at large Φ [55]. We note that we found that the polaron PA signal scales as $\Phi^{1/2}$ at large Φ in all the films we studied.

In order to identify the mechanism responsible for the PLDMR signal, we have explored the relation between N and δPL. Importantly, in figure 9 we see that $(\Delta T/T)^2$ coincides with high accuracy with the laser intensity dependence of δPL, i.e. $\delta PL \alpha N^2$. We have thus shown that the delayed PL is proportional to the recombination term in the polaron rate equation 1 and this relationship between δPL and N^2 directly implies that δPL is a result of a magnetic resonance effect on the non-geminate polaron recombination. The positive sign of the H-PLDMR then shows that the singlet exciton density is enhanced upon magnetic resonance.

2.1.3. Quantitative modelling of the spin-dependent recombination spectroscopy. We have seen that the PADMR and PLDMR spectra are in agreement with the qualitative expectations from a spin-dependent exciton formation model. Moreover a *quantitative* rate equation model has been developed [27, 29, 31] that allows determination of the value of r from the PADMR and PA spectra. The model starts from rate equations that describe the dynamics of the polaron, singlet and triplet exciton photoexcitations. Since polaron recombination and exciton formation are spin-dependent, two types of rate equations for each photoexcitation are needed: one describes the spin-dependent 'free' dynamics during the half-cycle of modulation when the microwave field is turned off, the other the dynamics under the boundary condition introduced by spin-1/2 magnetic resonance, i.e. that the pair densities of polarons recombining with parallel and antiparallel spins are equal. For simplicity these equations are written for steady state conditions $dn(t)/dt = 0$, i.e. the photoexcitation density is constant in time and given by the equilibrium obtained between photogeneration and spin-dependent recombination. In the previous paragraph we established that, under the present experimental conditions, polarons form non-geminate recombination pairs with their nearest neighbours and that their recombination rate is proportional to the total polaron density. Importantly our ODMR data imply that the recombination partners remain correlated with each other during most of their lifetime: if the polarons changed their recombination partner the spin polarization would be destroyed, since, on average, half of their new partners have parallel spin and half have antiparallel spin. Since after their formation the recombination kinetics of polaron pairs is not influenced by other polarons we therefore describe them using monomolecular kinetics, albeit with a recombination rate proportional to the total polaron density. Since the total polaron population changes little ($\delta N/N$ is typically 10%) we drop the explicit density dependence in the rate equations below. We note that the nature of the lifetime-long correlation of the non-geminately formed recombination pairs is presently not completely understood.

The general structure of the rate equations is as follows: the lhs is the change of the photoexcitation density with time (here set to zero because of steady state conditions), the first term on the rhs is the generation term as a result of laser photon absorption (Φ is the absorbed laser photon flux) and the last term on the rhs is the recombination term:

$$0 = \frac{\eta}{2}\Phi - R_P N_P \tag{2}$$

$$0 = \frac{\eta}{2}\Phi - R_{AP} N_{AP} \tag{3}$$

$$0 = \eta\Phi - \frac{R_P + R_{AP}}{2}\tilde{N}. \tag{4}$$

Equations (2) and (3) describe the spin-dependent polaron pair dynamics and (4) describes the dynamics under saturated resonance condition during the half-cycle of modulation when the microwave field is turned on. η is the photogeneration quantum efficiency for the polaron pairs. In equations (2) and (3), N_P and N_{AP} are the densities of parallel and antiparallel pairs, respectively, R_P and R_{AP} their respective recombination rates. In (4) $\tilde{N}$ is the total population under saturated spin-1/2 resonance conditions. We adopt the notation that densities under resonance conditions will be marked with a *tilde* sign. Equations (5) and (6) are the spin-dependent rate equations for singlet excitons:

$$0 = \eta_S \Phi + \frac{\sigma_S}{\sigma_S + \sigma_T} R_{AP} N_{AP} - \frac{N_S}{\tau_S} \tag{5}$$

$$0 = \eta_S \Phi + \frac{\sigma_S}{\sigma_S + 3\sigma_T} \frac{R_P + R_{AP}}{2} \tilde{N} - \frac{\tilde{N}_S}{\tau_S}. \tag{6}$$

Equation (5) expresses that singlet excitons, N_S, are generated directly upon laser photon absorption with quantum efficiency η_S but also as a result of delayed polaron recombination [56–58] (second term on the rhs). This so-called delayed singlet exciton formation rate is proportional to the polaron recombination term $R_{AP}N_{AP}$, since only antiparallel polaron pairs form singlet excitons. Antiparallel pairs can, however, also form a spin triplet configuration. We therefore have to introduce a weight term $\sigma_S/(\sigma_S + \sigma_T)$. τ_S is the singlet exciton lifetime. Equation (6) is the rate equation for singlets, $\tilde{N}_S$, under saturated magnetic resonance conditions. Analogous equations for the triplet excitons can be formulated. The solutions to the above rate equations are given in the form of a fractional change in population density upon spin-1/2 resonance:

$$\frac{\delta N}{N} = \frac{\delta T|_{P_1}}{\Delta T|_{P_1}} = -\left(\frac{r-1}{r+3}\right)^2 \tag{7}$$

$$\frac{\delta N_S}{N_S} = \frac{\delta T|_{S_1}}{\Delta T|_{S_1}} = \frac{\delta PL}{PL} = \frac{N_{S_{delayed}}}{N_S} \frac{r-1}{r+3} \tag{8}$$

$$\frac{\delta N_T}{N_T} = \frac{\delta T|_{T_1}}{\Delta T|_{T_1}} = -\frac{N_{T_{delayed}}}{N_T} \frac{r(r-1)}{(r+2)(r+3)}. \tag{9}$$

$N_{S_{delayed}}/N_S$ and $N_{T_{delayed}}/N_T$ measure the fraction of the delayed singlet and triplet excitons, respectively, that are produced from spin-dependent polaron recombination rather than by direct photogeneration. These fractions can be calculated from the rate equations and are functions of η, η_S and η_T. Most importantly, equation (7) allows determination of r from the experimentally obtained ratio $\delta T/\Delta T$ of polarons explicitly:

$$r = \sigma_S/\sigma_T = \frac{1 + 3(\delta T/\Delta T)^{1/2}}{1 - (\delta T/\Delta T)^{1/2}}. \tag{10}$$

Quantitative PA and PADMR experiments have been performed in a large number of materials [27, 29] with the goal of studying the material dependence of r.

2.1.4. Experimental checks. Before the results are summarized, we note that several experimental checks were performed on the mLPPP and PFO films (see [27], supplementary information) where we found that the condition of saturated magnetic resonance is indeed fulfilled in our ODMR experiments and that the r value obtained from the PA and PADMR experiments does not depend on the parameters chosen for the experiment (modulation frequencies, laser power and pump laser wavelength). $\delta T/\Delta T$ is also independent of temperature, which we checked for temperatures up to 160 K. At higher temperatures (typically

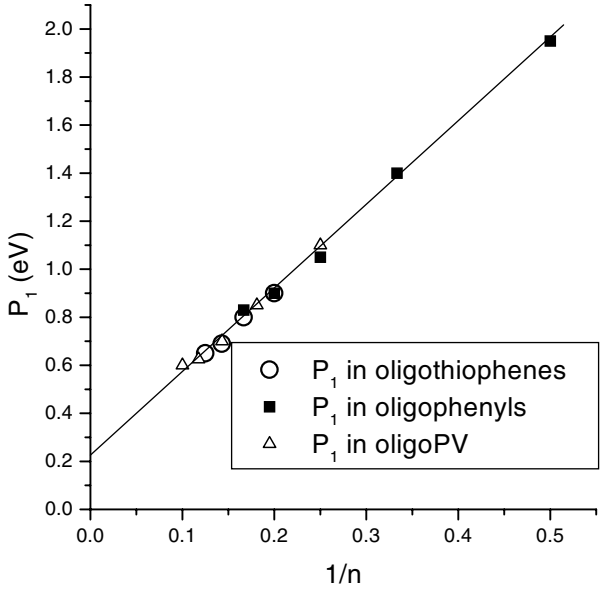

Figure 10. The peak photon energy of the low energy polaron transition, P_1, in singly oxidized oligomers as a function of the inverse CL. The number n denotes a CL that corresponds to an oligothiophene with n rings. The experimental data was taken from [60–62]. The line through the data points is a linear fit.

above 100 K) the polaron lifetime becomes too short, and in addition the PADMR signals become too weak for reliable measurements. However, since the extrapolation from 160 K to room temperature is not too great, we conclude that we expect that results from ODMR spectroscopy also apply to room temperature operation of OLED devices. We have also checked the independence of the r values obtained from the microwave frequency or applied magnetic field by comparing measurements on some of our films done in 3 and 16 GHz microwave resonators. Within experimental error, the results are identical for both microwave resonators [48].

2.1.5. Material dependence of spin-dependent exciton formation cross-sections. Understanding the material dependence of r is of great importance, since in principle it allows *a priori* selection of materials with large EL quantum efficiency in fluorescence based OLEDs. We note already at this point that the main result will be the discovery that r increases with the conjugation length (CL), where $r \approx 1$ in small molecules. The CL is the length over which the chemical conjugation and thus the extent of the π-electron wavefunctions are defect-free [59]; the CL is typically much shorter than the physical polymer chain length. We have shown that the CL in π-conjugated polymers can be measured spectroscopically [29]: figure 10 shows the dependence of the lower absorption band P_1 of polarons versus $1/\mathrm{CL}$ for a variety of singly oxidized oligomers [60–62]. It is seen that the absorption band P_1 depends linearly on $1/\mathrm{CL}$ irrespective of the π-conjugated backbone system. In fact, the dependence of P_1 on $1/\mathrm{CL}$ is universal and therefore can be used to infer the average CL of many π-conjugated polymer films. The polymer CL may therefore be deduced from the P_1 peak energy in the PA spectrum.

In figure 11 we show r as obtained from PADMR measurements in a large variety of π-conjugated materials versus P_1. Since P_1 is a linear function of $1/\mathrm{CL}$ we may actually

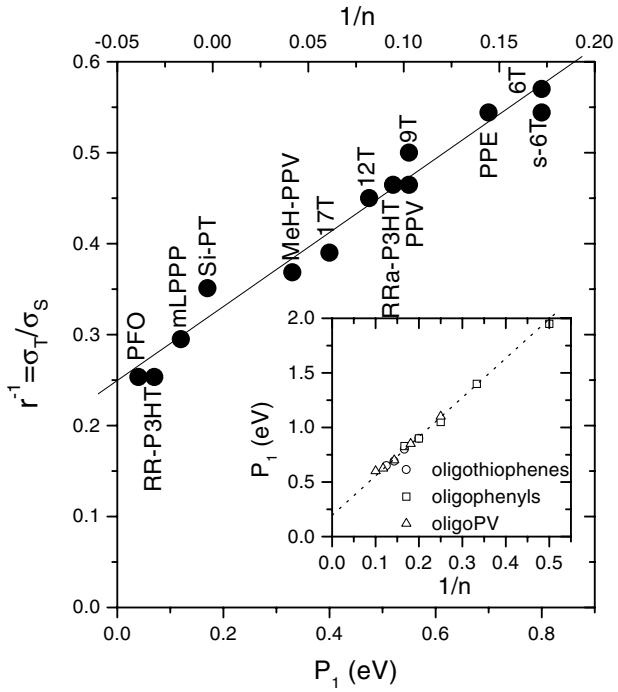

Figure 11. The ratio $r^{-1} = \sigma_T/\sigma_S$ of spin-dependent exciton formation cross-sections in various polymers and oligomers as a function of the peak photon energy of the P_1 transition (lower x axis). r^{-1} is also shown as a function of the inverse CL $1/n$ (upper x axis), which was determined from P_1 by linear extrapolation (see inset). The line through the data points is a linear fit. The inset shows the peak photon energy of the low energy polaron transition, P_1, in singly oxidized oligomers as a function of the inverse CL. The number n denotes a CL that corresponds to an oligothiophene with n rings. The experimental data was taken from [60–62]. The line through the data points is a linear fit.

plot r^{-1} versus $1/\mathrm{CL}$ as is also shown in figure 11 (upper axis). This uncovers a universal behaviour of $r(\mathrm{CL})$, namely that r^{-1} depends linearly on $1/\mathrm{CL}$ irrespective of the chain backbone structure, side groups or film morphology. The measured r values are apparently film morphology independent. This indicates that the recombination processes to form singlet and triplet excitons, respectively, depend on morphology in a similar way and that this dependence cancels out in measurements of the ratio r. We note that negative values for $1/\mathrm{CL}$ are encountered for several polymers that have the lowest P_1 transitions. In the present scheme these polymers would therefore be assigned a CL 'larger than infinity'. This situation was actually also encountered previously [63] in RR-P3HT, which was shown to form two-dimensional lamellae [63, 64]. It was indeed shown [63] that exceptionally low photon energy for the P_1 band results from a delocalization of polarons not only along the conjugated polymer backbone, but also in the two-dimensional structure perpendicular to the lamellae. This suggests an interpretation of the 'larger than infinite' CL as a situation where excitations extend not only along the backbone, but also along the perpendicular directions. It is, however, not entirely clear whether the linear extrapolation of the data presented in figure 10 to $1/\mathrm{CL} = 0$ is exactly valid. In any case polymers with a low P_1 band correspond to highly conjugated systems. In figure 11 we have adopted the notation that the number n denotes a CL that corresponds to an oligothiophene with n rings.

2.2. Singlet/triplet exciton ratio measured in working OLEDs

Wilson *et al* [28] have recently studied the singlet/triplet ratio directly in a working OLED. One of the two devices studied had a platinum-containing polymer as the active layer, whereas the other device contained the corresponding monomer (see [28] for the chemical and device structures). In their devices, the spin–orbit coupling introduced by the platinum atom allows triplet state emission, so optically and electrically generated luminescence from both singlet and triplet states could be directly compared.

The PL and EL spectra (figure 12) of the polymer and monomer measured by Wilson *et al* show two characteristic emission bands and the relative contribution of each band to the total emission is indicated as a percentage. In figure 12 the high and low energy bands are due to singlet and triplet excited states S_1 and T_1, respectively. It is seen that for electrical excitation Wilson *et al* observe a greater percentage of the photons to be from the triplet state, as expected since in PL originally only singlets are generated. For EL the excited state processes leading to emission are exactly the same as in PL, except that it is also possible to create triplet excitons directly. Wilson *et al* showed [28] that the absolute singlet generation fraction, χ_S, can be obtained from the spectra in figure 12 simply by

$$\chi_S = \frac{R_{PL}}{R_{EL}} \tag{11}$$

where R_{PL} is the ratio of triplet to singlet PL and R_{EL} is the analogous quantity for EL. They find an average singlet generation fraction of $22 \pm 1\%$ for the monomer device, but $57 \pm 4\%$ for the polymer device. This suggests that, in agreement with the results from magnetic resonance spectroscopy presented above, the recombination is spin-independent for the monomer, but that a spin-dependent process, favouring singlet formation, is effective in the polymer. Importantly, in additional experiments Wilson *et al* found that χ_S does not depend on the film thickness used in the device, or temperature, or the applied electric field (within the parameter range studied).

2.3. Conclusions from the experimental results

Wilson *et al* [28] employ the following argument to explain their observations: OLEDs operate by injection of electrons and holes from opposite electrodes and transport by hopping from one molecular site (or polymer chain) to the other. Electrons and holes capture one another when they are held within their mutually attractive potential; typical capture radii are about 10 nm. In this picture the distinction between molecular semiconductors and conjugated polymers is that this distance is considerably greater than a molecular dimension, but comparable to the delocalization lengths for electron and hole wavefunctions on polymer chains with large CL. Therefore, for molecular materials, electron/hole capture is achieved at a range where only the Coulomb interaction is effective, and the process is independent of the final spin state of the exciton. In contrast, for the polymers, when electron and hole are present on the same conjugation segment at the capture range, the interaction between them results also from direct overlap of electron and hole wavefunctions, and is therefore spin-dependent (through the exchange interaction). Thus, the probability of electron/hole capture is now spin-dependent. Wohlgenannt *et al* [29] remarked that the wavefunction extent of singlet excitons was measured to be as large as the CL [59]. In contrast, triplet excitons are always very confined: an average separation of electron and hole in the triplet state of PPV was measured to be $\approx$3.2 Å [65]. Therefore the difference between the singlet and triplet exciton wavefunctions significantly decreases with 1/CL [66] and this may explain the reason that r decreases with 1/CL. It appears that a complete description of spin-dependent exciton formation should include both a description of the electron/hole capture process and the spin-dependent exciton wavefunctions.

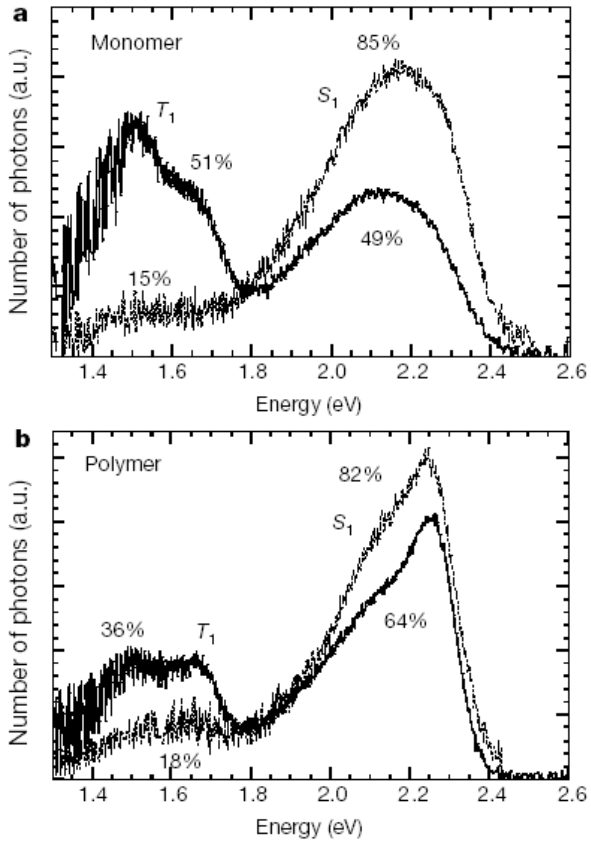

Figure 12. Comparison of the PL and EL spectra of light-emitting diodes of the platinum-containing polymer and monomer at 290 K. (a) The PL (dotted curve) and EL (full curve) spectra of a monomer LED. (b) The PL and EL spectra of a polymer LED. The triplet emission is denoted by T_1 and the singlet emission by S_1. The spectra have been plotted in terms of the number of photons and the fraction of the total emission that the singlet and triplet emission represent are given as percentages. Reprinted from [28].

3. Theoretical work

At first sight it is not too surprising that exciton formation in π-conjugated compounds is spin-dependent, given the large exchange energy that reduces the triplet exciton energy by typically 0.7 eV compared to that of the singlet exciton [19]. This is, however, only true for the lowest lying exciton levels, whereas for excited excitonic levels close to the continuum band, differences between singlet and triplet states are expected to be small. In this section we review the theoretical work on spin-dependent exciton formation.

The earliest theoretical work, by Shuai *et al* [18], considers that σ_S and σ_T are determined by intermolecular CT and recombination processes. Both contributions from the interchain hopping (interchain transfer integral, t^{perp}) and occupation-dependent hopping obtained from the bond-charge repulsion (off-diagonal interchain Coulomb repulsion, X^{perp}) are important and their relative strength determines the singlet fraction generated. Their main result, obtained by a molecular orbital perturbation approach, is shown in figure 13. The parameter of their model cannot be directly determined experimentally, making a direct comparison to

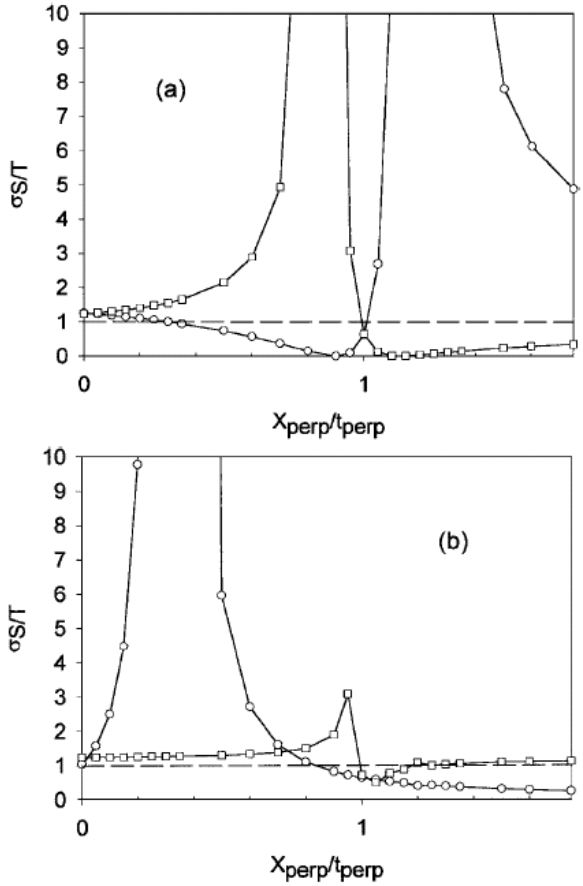

Figure 13. Evolution of the ratio between singlet exciton and triplet exciton formation cross sections $\sigma_{S/T}$ as a function of X/t: (a) in the case of weak coupling, circles for electron transport, squares for hole transport; and (b) in the coherent case (Davydov states), circles for optically active D1 state, squares for D2. Reprinted from [18].

experimental results difficult. In an extended manuscript Ye *et al* [67] study also the dependence of r on the CL and find that r increases with increasing CL for constant X^{perp}/t^{perp}.

Tandon *et al* [27] developed a theory that emphasizes the importance of the covalent or ionic nature of the bonds: singlet exciton formation is preferred because both the original pair of polarons and the final singlet exciton state are ionic in nature, whereas the triplet exciton is covalent. The terms 'ionic' and 'covalent' refer to an excited state where electron and hole excitations are located on different sites or on the same site on the conjugated backbone, respectively. In other words, in a covalent excitation the individual sites remain neutral, whereas in an ionic excitation sites can carry charge. Tandon *et al* use the (hypothetical) bond alternation parameter, δ [69], which is the normalized difference in length between single and double carbon bonds, to map more complicated π-conjugated systems onto polyacetylene, which is the simplest π-conjugated polymer also in terms of theoretical modelling. The exact quantum chemical model calculations, which were performed on short chain length oligomers rather than polymers, predict that r depends on δ in a systematic, but non-monotonic way [27]. Because there exists a direct relationship between δ and the compound's optical gap [69], this

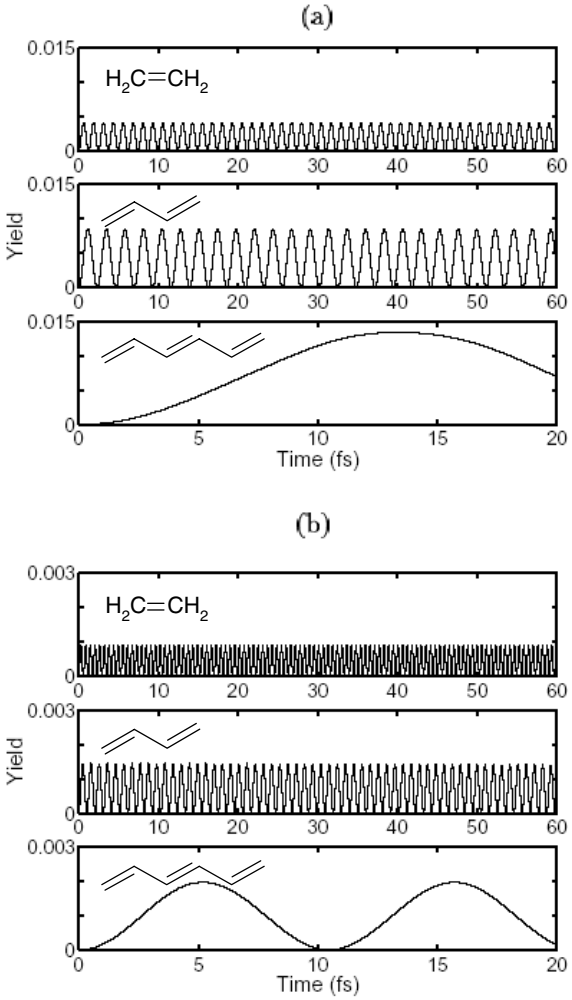

Figure 14. Yields in the singlet (a) and triplet (b) exciton formation channels within the two-chain PPP Hamiltonian with nonzero interchain hopping. In both (a) and (b) the top, middle and bottom panels are for pairs of ethylenes, butadienes and hexatrienes, respectively. The oscillations in the yields are analogous to Rabi oscillations; however, a transition to the final state occurs in the presence of radiative and non-radiative relaxations of singlet and triplet excitons, which damp the oscillations. From [68] with permission.

suggests that r may show a systematic dependence on the optical gap of the materials. In our early experiments we actually found that the measured r indeed depends on the optical gap in the materials we studied [27]. Later experiments [29], however, showed that the optical gap is apparently not the dominant parameter and that the CL is probably most important in determining the actual singlet fraction formed (see 2.1.5). In an extended manuscript Tandon *et al* [68] also investigate the dependence of r on the CL and achieve good qualitative agreement with our experimental data. Their calculations of r as a function of CL are done by exact quantum-chemical calculations in short oligomers (see figure 14). Calculations for longer CL are performed within a simplified formalism based on conclusions from the exact calculations. According to this formalism, the exciton formation rate can be obtained from the Schrödinger

equation that describes the direct transition from the state of separated polarons to the low lying exciton states, either spin singlet or spin triplet, due to a matrix element almost identical for both singlet and triplet channels. The spin-dependent yield therefore decreases with increasing energy difference, $\Delta E_{S(T)}$, between polaron pair and low lying exciton states. Now $\Delta E_S/\Delta E_T$ decreases with increasing CL (this follows from the ionic and covalent character of the low lying singlet and triplet exciton states, respectively) and therefore r increases with the CL.

Using a mixed quantum and classical molecular dynamics approach, Kobrak and Bittner [71] study the scattering of positive and negative polarons, which are already present on a single conjugation segment, into singlet and triplet excitons. Their model treats the particle–hole pair as a fully correlated two-particle quantum mechanical wavefunction, which interacts with a one-dimensional classical vibrational lattice. They find that the singlet exciton level is generally near resonance with the incident polaron pair, whereas this is not true for the triplet exciton levels. Singlet exciton formation is therefore preferred, as they find in their calculations. The energy mismatch of the triplet levels forces the triplet exciton to be formed in a state with high kinetic energy of the centre of mass motion, and the triplet exciton yield mostly depends on the density of states for the centre of mass motion. They find that r is mostly determined by the excitonic effective mass in such a way that small excitonic masses give the largest singlet/triplet ratio. We are not aware of any experimental data that probes the dependence of r on the effective mass. Karabunarliev and Bittner [72] perform similar calculations to study the dependence of r in their model on the CL. In a model system of PPV they find that r depends on the CL in a monotonic way (figure 15) such that r increases with CL in good agreement with our recent experimental data [29]. Their model calculations indicate that there are two types of essential states: band-like CT states and the low lying exciton states, the difference in energy between them being essentially the exciton binding energy. Now, in their model, exciton formation proceeds as a multi-pathway vibron-driven relaxation between the essential states, so that r is primarily determined by the triplet/singlet exciton binding energy ratio, which as their calculations show, depends on CL in a monotonic way. Tandon *et al* [68] have independently arrived at a similar result based on their calculation of intermolecular charge recombination.

Hong and Meng present a strikingly different view [73]: the singlet fraction is increased by ISC from the triplet manifold *after* formation of bound neutral excitons. The authors consider exciton formation as a cascade phonon emission process in which the energy of the electron–hole pair successively descends from the continuum to the bound states. ISC causes spin relaxation in addition to energy relaxation, and the spin relaxation is considered the origin of the enhanced singlet yield (see figure 16). According to this work ISC can become efficient in either of two cases:

(i) the exchange energy is small and back-transfer from the lowest triplet to the lowest singlet exciton state can occur since the lowest triplet state has long lifetime, or
(ii) the exchange energy is large and there is only a small number of triplet exciton levels; then the cooling of the initially formed triplet state is hindered by a phonon bottleneck and ISC can compete effectively with triplet exciton cooling.

In a PPV model these authors found that the singlet yield is large for an exchange gap larger than 0.8 eV or smaller than 0.3 eV. For intermediate exchange splittings the spin-statistical 25% should apply. Since the exchange energy in most π-conjugated polymers is $\approx$0.7 eV [19], the model by Hong and Meng requires that the density of triplet exciton states is very small, resulting in a phonon bottleneck for triplet exciton cooling. To the best of our knowledge the density of triplet states has not been unambiguously determined by experiment.

We therefore conclude that a commonly agreed theoretical picture has not yet emerged.

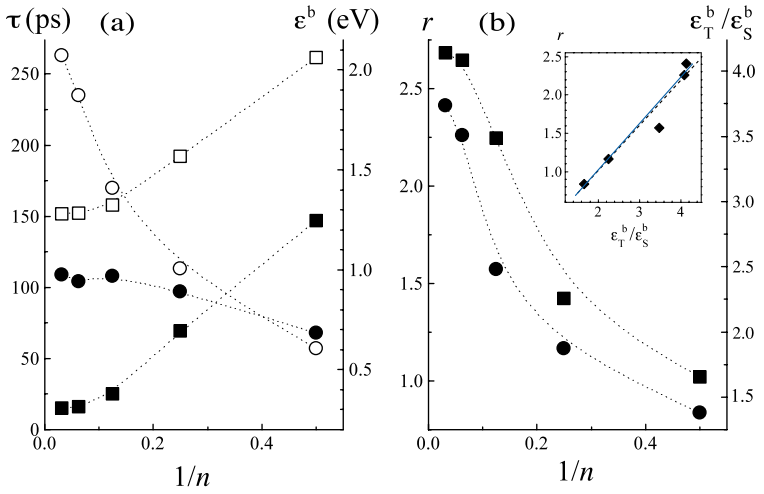

Figure 15. (a) Variation of singlet and triplet binding energies and formation times with inverse CL $1/n$. (τ_S—●, τ_T—○, ϵ_S^b—■, ϵ_T^b—□). (b) Formation-time ratio $r = \tau_T/\tau_S$ (●) and binding-energy ratio $\epsilon_S^b/\epsilon_T^b$ (■) versus $1/n$. Inset: r versus $\epsilon_T^b/\epsilon_S^b$. Broken curves are guides for the eye. Reprinted from [70].

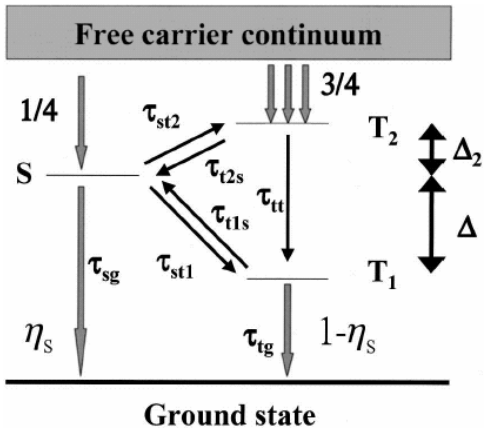

Figure 16. The relevant transitions are shown with their transition lifetimes. S and T_2 excitons come from the continuum with ratio 1:3. After the possible intertransitions, all excitons must recombine through either the τ_{sg} or the τ_{tg} channel. The intrinsic yield η_s is defined as the fraction of the recombinations through the τ_{sg} channel. Reprinted from [73].

4. Conclusions

We conjecture that the experimental findings show that the CL of the π-conjugated compound is the most important parameter determining the ratio r of spin-dependent exciton formation cross-sections and therefore also the singlet/triplet ratio. In particular, it follows that, if all other factors are equal, π-conjugated polymer devices should be able to reach higher efficiencies when compared to small molecular devices, unless triplet harvesting schemes are employed. On the other hand, a commonly agreed theoretical picture has not yet emerged. Different theoretical models for the spin-dependent exciton formation do not yet agree on which mechanism determines the singlet/triplet ratio.

Acknowledgments

We thank S Mazumdar for many useful and stimulating discussions and X M Jiang and C Yang for their invaluable contributions in the course of the measurements. This work was supported in part by DOE ER-45490 and NSF DMR-02-02790

Appendix. η_{max} determination

We have performed rate equation calculations at steady state conditions to demonstrate how the ratio $r = \sigma_S/\sigma_T$ determines the maximum EL quantum efficiency, η_{max}, in the presence of competing processes such as spin–lattice relaxation. These calculations start from the rate equation for the polaron pairs and their final result is η_{max}.

There are four possible spin configurations, namely antiparallel (AP) spins in singlet configuration (APS), AP in triplet configuration (APT) and two configurations for parallel spins (P). We use a steady state rate equation for each configuration. The two rate equations for the two P configurations are, however, identical, so that three rate equations are sufficient:

$$\frac{\mathrm{d}N_P}{\mathrm{d}t} = \frac{I\eta_3}{2} - k_T N_P - k_{SL}(N_P - N/2) = 0 \tag{A.1}$$

$$\frac{\mathrm{d}N_{APS}}{\mathrm{d}t} = \frac{I\eta_3}{4} - k_S N_{APS} - k_{SL}(N_{APS} - N/4) = 0 \tag{A.2}$$

$$\frac{\mathrm{d}N_{APT}}{\mathrm{d}t} = \frac{I\eta_3}{4} - k_T N_{APT} - k_{SL}(N_{APT} - N/4) = 0. \tag{A.3}$$

Here N_P, N_{APS}, N_{APT} are the density of P, APS and APT pairs, N is their sum, I is the current, η_3 gives the fraction of the injected charges that form e–h pairs, k_S and k_T are the formation rates of singlet and triplet excitons from the CT reaction (these rates are proportional to σ_S and σ_T, respectively) and k_{SL} is the spin–lattice relaxation rate. The first terms on the right-hand side of the rate equations describe the formation of e–h pairs from the injected current, whereas the second term gives the recombination of the e–h pairs to either singlet (APS) or triplet (APT, P) excitons. Spin-lattice relaxation is introduced by the last term, which relaxes the system back to equilibrium, where each of the four configurations has equal probability.

The steady state singlet exciton population, N_{SE}, may then be obtained from the following rate equation:

$$\frac{N_{SE}}{\mathrm{d}t} = k_S N_{APS} - N_{SE}/\tau_{SE} = 0 \tag{A.4}$$

where τ_{SE} is the singlet exciton lifetime. N_{APS} was obtained as a solution of equations (A.2)–(A.3). Finally η_{EL} is given by $(N_{SE}/\tau_{SE})(\eta_{PL}/I)$, where η_{PL} is the photoluminescence quantum efficiency. Furthermore $\eta_{max} = \eta_{EL}/(\eta_3\eta_{PL})$, for which we obtained the following expression:

$$\eta_{max} = \frac{k_S(k_T + k_{SL})}{4k_S k_T + k_S k_{SL} + 3k_T k_{SL}}. \tag{A.5}$$

Of special interest are the limiting values of η_{max} for $k_{SL} = 0$ on the one hand and k_{SL} much larger than k_S on the other hand:

$$\eta_{max} \overset{k_{SL}=0}{\longrightarrow} 1/4 \tag{A.6}$$

$$\eta_{max} \overset{k_{SL}\gg k_S}{\longrightarrow} \frac{k_S/k_T}{k_S/k_T + 3} = \frac{r}{r+3}. \tag{A.7}$$

We note that the above result (A.7) is quite general and is not restricted to a situation with efficient spin–lattice relaxation. In the presence of any effective channel competing with charge recombination, η_{max} is given by (A.7). We note that, to the best of our knowledge, such competing channels have not yet been explicitly identified in OLEDs. Potential candidates include spin–orbit coupling, spin-dependent e–h capture radii or the competition between exciton cooling rate and exciton dissociation by the electric field.

References

[1] Friend R H, Gymer R W, Holmes A B, Burroughes J H, Marks R N, Taliani C, Bradley D D C, Santos D A D, Brédas J L, Löglund M and Salaneck W R 1999 Electroluminescence in conjugated polymers *Nature* **397** 121–8

[2] Pope M, Kallmann H and Magnante P 1963 *J. Chem. Phys.* **38** 2042

[3] Helfrich W and Schneider W G 1965 *Phys. Rev. Lett.* **14** 229

[4] Tang C W and Van Slyke S A 1987 Organic electroluminescent diodes *Appl. Phys. Lett.* **51** 913–15

[5] Chiang C K, Fincher C R Jr, Park Y W, Heeger A J, Shirakawa H, Louis E J, Gau S C and MacDiarmid A G 1977 Electrical conductivity in doped polyacetylene *Phys. Rev. Lett.* **39** 1098–101

[6] Garnier F, Hajlaoui R, Yassar A and Srivastava P 1994 All-polymer field-effect transistor realized by printing techniques *Science* **265** 1684–6

[7] Torsi L, Dodabalapur A, Rothberg L J, Fung A W and Katz H E 1996 Intrinsic transport properties and performance limits of organic field-effect transistors *Science* **272** 1462

[8] Yang Y and Heeger A J 1994 A new architecture for polymer transistors *Nature* **372** 344–6

[9] Brown A R, Pomp A, Hart C M and Deleeuw D M 1995 Logic gates made from polymer transistors and their use in ring oscillators *Science* **270** 972

[10] Sirringhaus H, Tessler N and Friend R H 1998 Integrated optoelectronic devices based on conjugated polymers *Science* **280** 1741–4

[11] Yu G, Gao J, Hummelen J C, Wudl F and Heeger A J 1995 Polymer photovoltaic cells: enhanced efficiencies via a network of internal donor–acceptor heterojunctions *Science* **270** 1789

[12] Granström M, Petritsch K, Arias A C, Lux A, Anderson M R and Friend R H 1998 Laminated fabrication of polymeric photovoltaic diodes *Nature* **395** 257–60

[13] Burroughes J H, Bradley D D C, Brown A R, Marks R N, Mackay K, Friend R H, Burn P L and Holmes A B 1990 Light-emitting-diodes based on conjugated polymers *Nature* **347** 539–41

[14] Burn P L, Holmes A B, Kraft A, Bradley D D C, Brown A R, Friend R H and Gymer R W 1992 Chemical tuning of electroluminescent copolymers to improve emission efficiencies and allow patterning *Nature* **356** 47–9

[15] Greenham N C, Moratti S C, Bradley D D C, Friend R H and Holmes A B 1993 Efficient light-emitting-diodes based on polymers with high electron-affinities *Nature* **365** 628–30

[16] Braun D and Heeger A J 1991 Visible-light emission from semiconducting polymer diodes *Appl. Phys. Lett.* **58** 1982–4

[17] Gustafsson G, Cao Y, Treacy G M, Klavetter F, Colaneri N and Heeger A J 1992 Flexible light-emitting-diodes made from soluble conducting polymers *Nature* **357** 477–9

[18] Shuai Z, Beljonne D, Silbey R J and Brédas J L 2000 Singlet and triplet exciton formation rates in conjugated polymer light-emitting diodes *Phys. Rev. Lett.* **84** 131–4

[19] Köhler A, Wilson J S and Friend R H 2002 Fluorescence and phosphorescence in organic materials *Adv. Mater.* **14** 701–7

[20] Baldo M A, O'Brien D F, Thompson M E and Forrest S R 1999 Excitonic singlet-triplet ratio in a semiconducting organic thin film *Phys. Rev.* B **60** 14422–8

[21] Baldo M A, Thompson M E and Forrest S R 2000 High-efficiency fluorescent organic light-emitting devices using a phosphorescent sensitizer *Nature* **403** 750–3

[22] Adachi C, Baldo M A, Thompson M E and Forrest S R 2001 Nearly 100% internal phosphorescence efficiency in an organic light-emitting device *J. Appl. Phys.* **90** 5048–51

[23] Lupton J M, Pogantsch A, Piok T, List E J W, Patil S and Scherf U 2002 Intrinsic room-temperature electrophosphorescence from a pi-conjugated polymer *Phys. Rev.* B **65** 045208–045208/13

[24] Cao Y, Parker I D, Yu G, Zhang C and Heeger A J 1999 Improved quantum efficiency for electroluminescence in semiconducting polymers *Nature* **397** 414–17

[25] Ho P K H, Kim J, Burroughes J H, Becker H, Li S F Y, Brown T M, Cacialli F and Friend R H 2000 Molecular-scale interface engineering for polymer light-emitting diodes *Nature* **404** 481–4

[26] Sariciftci N S (ed) 1997 *Primary Photoexcitations in Conjugated Polymers; Molecular Excitons versus Semiconductor Band Model* (Singapore: World Scientific)
[27] Wohlgenannt M, Tandon K, Mazumdar S, Ramasesha S and Vardeny Z V 2001 Formation cross-sections of singlet and triplet excitons in pi-conjugated polymers *Nature* **409** 494–7
[28] Wilson J S, Dhoot A S, Seeley A J A B, Khan M S, Köhler A and Friend R H 2001 Spin-dependent exciton formation in pi-conjugated compounds *Nature* **413** 828–31
[29] Wohlgenannt M, Jiang X M, Vardeny Z V and Janssen R A J 2002 Conjugation-length dependence of spin-dependent exciton formation rates in pi-conjugated oligomers and polymers *Phys. Rev. Lett.* **88** 197401–4
[30] Dhoot A S, Ginger D S, Beljonne D, Shuai Z and Greenham N C 2002 Triplet formation and decay in conjugated polymer devices *Chem. Phys. Lett.* **360** 195–201
[31] Wohlgenannt M, Yang C and Vardeny Z V 2002 Spin-dependent delayed luminescence from non-geminate pairs of polarons in pi-conjugated polymer films *Phys. Rev.* B at press
[32] Greenham N C, Shinar J, Partee J, Lane P A, Amir O, Lu F and Friend R H 1996 Optically detected magnetic resonance study of efficient two-layer conjugated polymer light-emitting diodes *Phys. Rev.* B **53** 13528–33
[33] Sariciftci N S, Smilowitz L, Heeger A and Wudl F 1992 Photoinduced electron-transfer from a conducting polymer to buckminsterfullerene *Science* **258** 1474–6
[34] Vardeny Z V and Wei X 1997 *Handbook of Conducting Polymers* vol 2 (New York: Marcel) ch 22
[35] Graupner W, Meghdadi F, Leising G, Lanzani G, Nisoli M, Silvestri S D, Fischer W and Stelzer F 1997 Photoexcitations in para-hexaphenyl *Phys. Rev.* B **56** 10128–32
[36] Comoretto D, Moggio I, Cuniberti C, Musso G F, Dellepiane G, Borghesi A, Kajzar F and Lorin A 1998 Long-lived photoexcited states in polydiacetylenes: the photoinduced-absorption spectra of pda-4bcmu *Phys. Rev.* B **57** 7071–8
[37] Epshtein O, Nakhmanovich G, Eichen Y and Ehrenfreund E 2001 Dispersive dynamics of photoexcitations in conjugated polymers measured by photomodulation spectroscopy *Phys. Rev.* B **63** 125206–11
[38] List E J W, Partee J, Shinar J, Scherf U, Müllen K, Zojer E, Petritsch K, Leising G and Graupner W 2000 Localized triplet excitations and the effect of photo-oxidation in ladder-type poly(p-phenylene) and oligo(p-phenylene) *Phys. Rev.* B **61** 10807–14
[39] Ago H, Shaffer M S P, Ginger D S, Windle A H and Friend R H 2000 Electronic interaction between photoexcited poly(p-phenylene vinylene) and carbon nanotubes *Phys. Rev.* B **61** 2286–90
[40] Frolov S V, Kloc C, Batlogg B, Wohlgenannt M, Jiang X and Vardeny Z V 2001 Excitation dynamics in single molecular crystals of α-hexathiophene from femtoseconds to milliseconds *Phys. Rev.* B **63** 205203–14
[41] Janssen R A J, Sariciftci N S and Heeger A J 1995 Triplet-state photoexcitations and triplet-energy transfer in poly(3-alkylthiophene) C_{60} solutions *Synth. Met.* **70** 1343–4
[42] Scherf U and Müllen K 1991 Polyarylenes and poly(arylenevinylenes).7. a soluble ladder polymer via bridging of functionalized poly(para-phenylene)-precursors *Makromol. Chem.* **12** 489–97
[43] Wei X, Hess B C, Vardeny Z V and Wudl F 1992 Studies of photoexcited states in polyacetylene and poly(paraphenylenevinylene) by absorption detected magnetic resonance: the case of neutral photoexcitations *Phys. Rev. Lett.* **68** 666–9
[44] Lane P A, Wei X and Vardeny Z V 1997 Spin and spectral signatures of polaron pairs in pi-conjugated polymers *Phys. Rev.* B **56** 4626–37
[45] Leng J M, Wei X, Vardeny Z V, Khemani K C, Moses D and Wudl F 1993 Magneto-optical studies of photoexcitations in C_{61} *Phys. Rev.* B **48** 18250–3
[46] Wei X, Vardeny Z V, Sariciftci N S and Heeger A J 1996 Absorption-detected magnetic-resonance studies of photoexcitations in conjugated-polymer/C_{60} composites *Phys. Rev.* B **53** 2187–90
[47] Lane P A, Wei X and Vardeny Z V 1996 Studies of charged excitations in pi-conjugated oligomers and polymers by optical modulation *Phys. Rev. Lett.* **77** 1544–7
[48] Wei X 1996 *PhD Thesis* University of Utah
[49] Depinna S, Cavenett B C, Austin I G, Searle T M, Thompson M J, Allison J and Lecomber P G 1982 Characterization of radiative recombination in amorphous-silicon by optically detected magnetic-resonance.1. *Phil. Mag.* B **46** 473–500
[50] Swanson L S, Shinar J and Yoshino K 1990 Optically detected magnetic resonance study of polaron and triplet-exciton dynamics in poly(3-hexylthiophene) and poly(3-dodecylthiophene) films and solutions *Phys. Rev. Lett.* **65** 1140–3
[51] Boulitrop F 1983 Recombination processes in a-Si: H. a study by optically detected magnetic resonance *Phys. Rev.* B **28** 6192–208
[52] Lane P A, Swanson L S, Ni Q-X, Shinar J, Engel J P, Barton T J and Jones L 1992 Dynamics of photoexcited states in C_{60}: an optically detected magnetic resonance, ESR, and light-induced ESR study *Phys. Rev. Lett.* **68** 887–90

[53] List E J W, Kim C-H, Naik A K, Scherf U, Leising G, Graupner W and Shinar J 2001 Interaction of singlet excitons with polarons in wide band-gap organic semiconductors: a quantitative study *Phys. Rev.* B **64** 155204–11
[54] Korovyanko O J and Vardeny Z V 2002 Film morphology and ultrafast photoexcitation dynamics in polyfluorene *Chem. Phys. Lett.* **356** 361–7
[55] Wohlgenannt M, Graupner W, Leising G and Vardeny Z V 1999 Photogeneration and recombination processes of neutral and charged excitations in films of a ladder-type poly(para-phenylene) *Phys. Rev.* B **60** 5321–30
[56] Romanovskii Y V, Gerhard A, Schweitzer B, Personov R I and Bässler H 1999 Delayed luminescence of the ladder-type methyl-poly(para-phenylene) *Chem. Phys. Lett.* **249** 29–39
[57] Schweitzer B, Arkhipov V I, Scherf U and Bässler H 1999 Geminate pair recombination in a conjugated polymer *Chem. Phys. Lett.* **313** 57–62
[58] Hertel D, Bassler H, Guentner R and Scherf U 2001 Triplet-triplet annihilation in a poly(fluorene)-derivative *J. Chem. Phys.* **115** 10007–13
[59] Knupfer M, Fink J, Zojer E, Leising G and Fichou D 2000 Universal exciton size scaling in pi conjugated systems *Chem. Phys. Lett.* **318** 585–9
[60] Khanna R K, Jiang Y M, Srinivas B, Smithhart C B and Wertz D L 1993 Electronic-transitions in polarons and bipolarons of poly(p-phenylene) oligomers *Chem. Mater.* **5** 1792–8
[61] Guay J, Kasai P, Diaz A, Wu R L, Tour J M and Dao L H 1992 Chain-length dependence of electrochemical and electronic-properties of neutral and oxidized soluble alpha,alpha-coupled thiophene oligomers *Chem. Mater.* **4** 1097–105
[62] Schenk R, Gregorius H and Müllen K 1991 Absorption-spectra of charged oligo(phenylenevinylene)s—on the detection of polaronic and bipolaronic states *Adv. Mater.* **3** 492–3
[63] Österbacka R, An C P, Jiang X M and Vardeny Z V 2000 Two-dimensional electronic excitations in self-assembled conjugated polymer nanocrystals *Science* **287** 839–42
[64] Sirringhaus H, Brown P J, Friend R H, Nielsen M M, Bechgaard K, Langeveld-Voss B M W, Spiering A J H, Janssen R A J, Meijer E W, Herwig P and de Leeuw D M 1999 Two-dimensional charge transport in self-organized, high-mobility conjugated polymers *Nature* **401** 685–8
[65] Österbacka R, Wohlgenannt M, Chinn D and Vardeny Z V 1999 Optical studies of triplet excitations in poly(p-phenylene vinylene) *Phys. Rev.* B **60** R11253–6
[66] Pedersen T G, Johansen P M and Pedersen H C 2000 Particle-in-a-box model of one-dimensional excitons in conjugated polymers *Phys. Rev.* B **61** 10504–10
[67] Ye A, Shuai Z and Brédas J L 2002 Coupled-cluster approach for studying the singlet and triplet exciton formation rates in conjugated polymer led's *Phys. Rev.* B **65** 045208–045208/13
[68] Tandon K, Ramasesha S and Mazumdar S 2002 Electron correlation effects in electron–hole recombination in organic light-emitting diodes *Phys. Rev.* B at press
[69] Soos Z G, Ramasesha S and ao D S G 1993 Band to correlated crossover in alternating hubbard and pariser-parr-pople chains: nature of the lowest singlet excitation of conjugated polymers *Phys. Rev. Lett.* **71** 1609–12
[70] Karabunarliev S and Bittner E R 2002 Spin-dependent electron–hole capture kinetics in conjugated polymers *Phys. Rev.* B at press
[71] Kobrak M N and Bittner E R 2000 Quantum molecular dynamics study of polaron recombination in conjugated polymers *Phys. Rev.* B **62** 11473–86
[72] Karabunarliev S and Bittner E R 2002 Spin-dependent electron–hole capture kinetics in conjugated polymers *Preprint* cond-mat/0206499
[73] Hong T and Meng H 2001 Spin-dependent recombination and electroluminescence quantum yield in conjugated polymers *Phys. Rev.* B **63** 075206–075206/5